Chapter 4

Crystal interface and microstructure

4.1 Surface tension at interface

A theoretically infinite system has no interfaces. However, every system we are interested in engineering has a finite size. Even if it is very large. To have a finite size is to have an end, which in other words means to have an interface. From a thermodynamic point of view, there is an interface energy that corresponds to an interface. Assuming Gibbs free energy G_0 of the system that does not consider the interface, the free energy G of the system when the interface is considered is given as follows.

$$G = G_0 + A\gamma$$

where A is area of interface and γ is interface energy per area. Then, we have

$$dG = \gamma dA + Ad\gamma$$

Since the interface has excess energy, the surface tension is applied when the area of surface changes,

$$\mathbf{F} = -\frac{\partial G}{\partial A}\hat{n}$$

and it acts inwardly, towards the body of the object where $\hat{n}$ is surface(interface) normal(outward). Therefore,

$$F = |\mathbf{F}| = \frac{\partial G}{\partial A} = \gamma$$

which the unit of surface tension is

$$\frac{\text{J}}{\text{m}^2} = \frac{\text{N}}{\text{m}}$$

4.2 Interface shape

4.2.1 Gibbs-Wulff theorem

When there are many segments of interface, we can represent the interface energy by
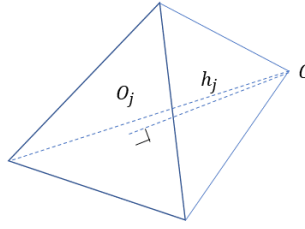
$$G_i = \sum_j \gamma_j O_j$$

Figure 4.1: The triangular pyramid which consists of three points at interface segment and center of the crystal.

where γ_j is interface energy of j-th segment and O_j is the area for j-th segment. In Fig. 4.1 At given volume, assuming that γ_j is predetermined,

$$\delta\left(\sum_j \gamma_j O_j\right)_V = \sum_j \gamma_j \delta O_j = 0$$

If you connect each vertex of the interface segment (assuming it is a triangle) from the center of the crystal, a triangular pyramid will come out. Draw a line perpendicular to the interface segment from the center and let the distance be h_j. Since the volume

$$V = \frac{1}{3}\sum_j O_j h_j$$

Then we have

$$\delta V = \frac{1}{3}\sum_j \left[\delta O_j h_j + O_j \delta h_j\right] = 0$$

When we assume that h_j is also constant, we have that

$$\sum_j \delta O_j h_j = 0$$

to make the volume conserved. For the interface energy minimization,

$$\sum_j \delta O_j \gamma_j = 0$$

To make the both conditions true, the case is

$$h_j = \lambda \gamma_j$$

therefore, we found that when h_j is proportional to the γ_j, the interface energy is minimized at given volume.

If the surface tension depends on the direction, the process depicted in Fig. 4.2, we can predict the equilibrium shape of domain. The equilibrium shape (blue line) in Fig. 4.2 is known as Wulff construction.

4.3 Boundaries in Single-phase solids

Single phase materials are homogeneous in composition. However, even excluding the surface, there are many boundaries within it, which is the boundary that separates two regions with different crystallographic orientations, which is called a grain
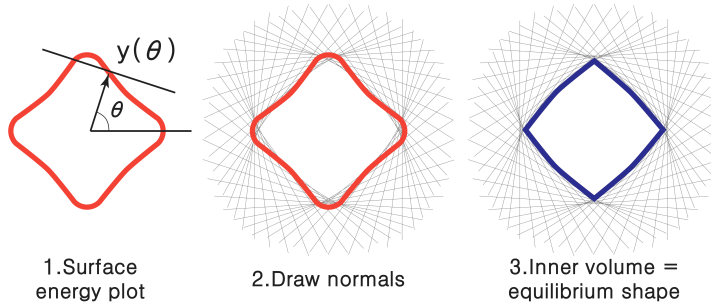
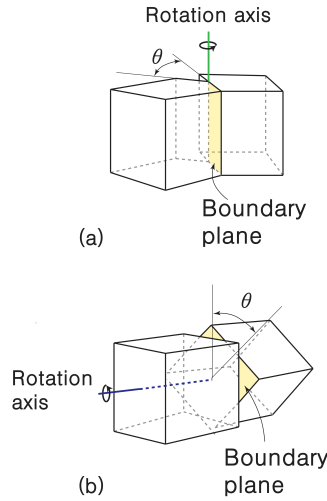Figure 4.2: Schematic procedure to construct Wulff construction.

Figure 4.3: The relative orientations of the crystals and the boundary forming (a) a tilt boundary (b) a twist boundary.

boundary. In other words, a region with the same crystallographic orientation is called a grain. The properties of this interface are very important for predicting the properties of materials. There is a very large amount of content here, and this course aims to examine some of the central theories.

4.3.1 Low angle grain boundary

Low angle boundary means a boundary formed by two grains with a small difference in crystallographic orientation. There are two types of low angle boundaries, tilt boundary and twist boundary as shown in Fig. 4.3. Typically, we classify the boundary as low angle grain boundary (LAGB) when misfit angle is lower than 10°-15°. Low angle grain boundaries are usually described as periodic arrays of edge dislocations. The spacing of dislocations in Fig. 4.4 is

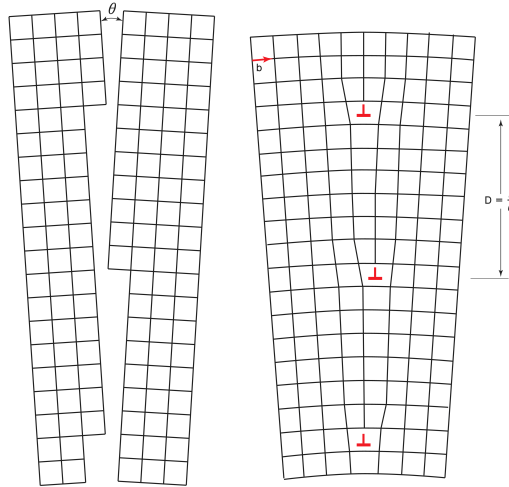$$D = \frac{b}{\sin \theta} \simeq \frac{b}{\theta}$$

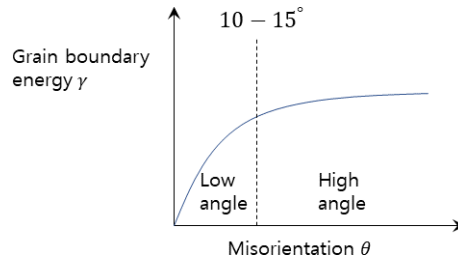Figure 4.4: (a) Low-angle tilt boundary. (b) Low-angle twist boundary.

Figure 4.5: Variation of grain boundary energy with misorientation θ

When D is very large (small θ) the grain boundary energy is proportional to the misfit angle

$$\gamma \propto \theta$$

As D decreases, the strain fields for each dislocation cancel out so that γ increases at a decreasing rate in Fig. 4.5.

4.4   High angle grain boundary

For high angle grain boundary, atomic structure is not fully understand so far. Still many debating, and we generally assume that the grain boundary energy is relatively constant with respect to the misorientation angle. A high angle grain boundary (HAGB) has open structure and it generally have higher grain boundary energy comparing to the LAGB. However, in some special cases, there are cases where the grain boundary energy is much lower than that of the random boundary, and a twin boundary exists typically.

4.4.1   Special high grain boundary

As shown in Fig. 4.6, a coherent twin boundary has significantly low energy comparing to the incoherent twin boundary.   Twin orientation in FCC metals correspond
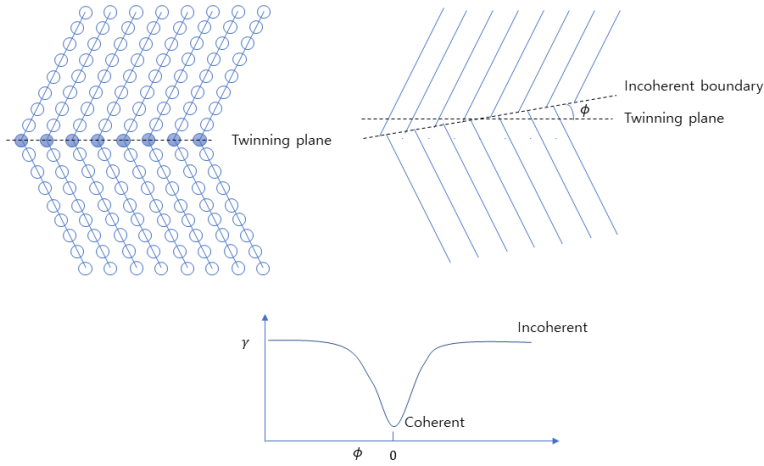
Figure 4.6: Coherent and incoherent twin boundary. Twin boundary energy as a function of the misorientation.

Crystal	CTBE	ITBE	GBE
Cu	21	498	623
Ag	8	126	377
Fe-Cr-Ni (SS304)	19	209	835

Table 4.1: CTBE(Coherenet Twin Boundary energy), ITBE(Incoherenet Twin Boundary energy), GBE(Grain boundary energy).

to a misorientation of 70.5° about $\langle 110 \rangle$ axis. A measured grain boundary energy function of misorientation is shown in Fig. 4.7.

4.5   Grain growth

4.5.1   Force balance at triple junction

When three different grain boundaries meet at a triple junction as shown in Fig. 4.8, the relationship between grain boundary energies are

$$\frac{\gamma_1}{\sin \theta_1} = \frac{\gamma_2}{\sin \theta_2} = \frac{\gamma_3}{\sin \theta_3}$$

When grain boundary energy is isotropic ($\gamma_1 = \gamma_2 = \gamma_3$),

$$\theta_1 = \theta_2 = \theta_3 = 120°$$

4.5.2   Stable configuration of grains in 2D with isotropic grain boundary energy

As numbers of neighboring grains are from 3, 4, 6 and 7, to meet the 120° condition, the boundary have to be convex or concave without the case when number of neighboring grains is 6 in Fig. 4.9. We can generally say, when the grain boundary energy is isotropic,
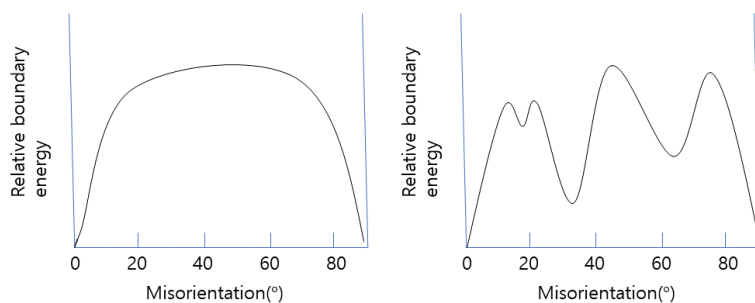
$$\frac{dA}{dt} = k(n - 6)$$

Figure 4.7: Schematic grain boundary energies for symmetric tilt boundaries in Al (a) when the rotation axis is parallel to (100), (b) when the rotation axis is parallel to (110).
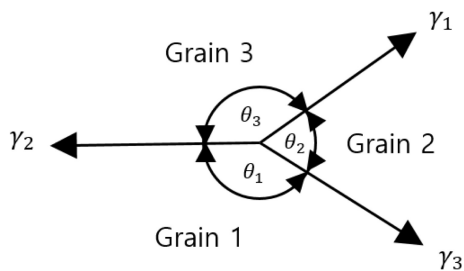

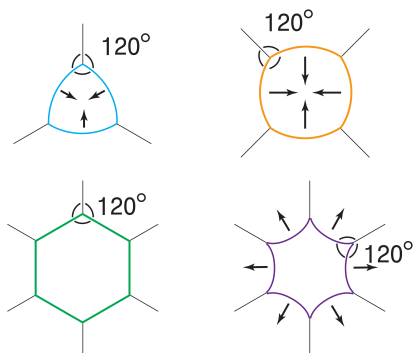Figure 4.8: The balance of grain boundary energy at triple junction

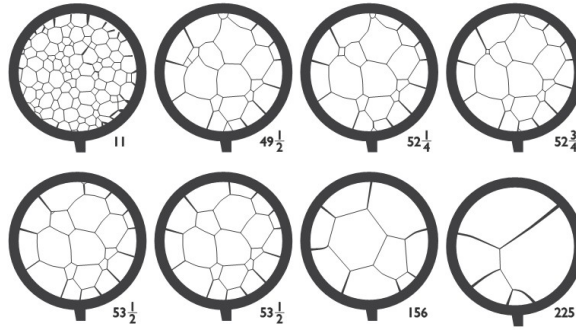Figure 4.9: Two dimensional grain boundary configurations.

Figure 4.10: Two-dimensional cells of a soap solution illustrating the process of grain growth. Numbers are time in minutes.
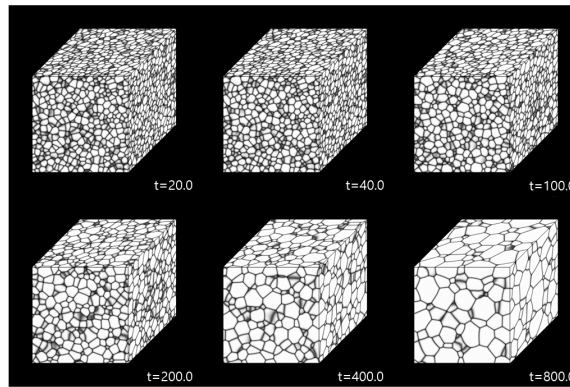

Figure 4.11: 3D grain structure obtained from the phase-field modeling.

when A is grain area an n is number of neighboring grains in two-dimensional system. We say the relation is von Neumann-Mullins relation.

4.5.3   Grain growth kinetics

As illustrated in Fig. 4.10, average area of soap bubble increases as time evolves. The grain growth means the phenomena where average grain size increases as time proceeds. The main driving force of the grain growth is the grain boundary energy minimization. Small grains eliminate and larges grains are getting bigger. Since the chemical potential difference by the surface tension is described by Gibbs-Thomson effect which is

$$\Delta\mu = \Delta G = \frac{2\gamma V_m}{r}$$

where γ is the surface tension and r is radius of the grain. Once the grain becomes, chemical potential increases, therefore, the grain becomes highly unstable. The overall kinetics can be evaluated

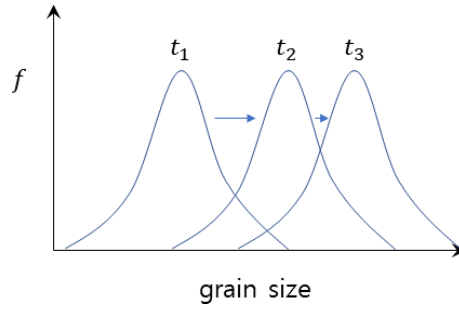$$\frac{dD}{dt} = \alpha M \frac{2\gamma}{D} \to D^2 = D_0^2 + 4\alpha M t$$

Figure 4.12: Frequency with respect to grain size at different time t_1, t_2, t_3

4.5.4 Self-similarity

Although not strictly scientifically proven, it is assumed that the size of grains in the microstructure in which grain growth occurs are not all the same, and their distribution has a consistent shape with time. However, it is explained that the average grain size increases with time as shown in Fig. 4.12.

4.5.5 Mean field approach proposed by Hillert

n is average number of neighboring grains (sides) in 2D,

$$n = 6 + 6\alpha \left(\frac{R}{R_{cr}} - 1 \right)$$

where R is size of grain. When

$$R > R_{cr}$$

the grain growth and when

$$R < R_{cr}$$

grain shrinks. Of course it is simplified approach and we say it is mean-field approach. However, full-scale complex system consideration is too challenging. After some calculation,

$$\frac{du^2}{d\tau} = \gamma(u - 1) - u^2$$

where

$$u = \frac{R}{R_{cr}}$$

$$\gamma = 2\alpha M \sigma (dt/dR_{cr}^2)$$

$$\tau = \ln R_{cr}^2$$

The the probability distribution function is

$$P(u) = \frac{\beta u}{(2 - u)^{2+\beta}} (2e)^\beta \exp \left(-\frac{2\beta}{2 - u} \right)$$

For two-dimensional system $\beta = 2$ and three-dimensional system $\beta = 3$. After some more treatment, we can get frequency $f(\rho)$ in 2-D function of $\rho = r/<r>$.

$$f(\rho) = \frac{2^3 e^2 \rho}{(2 - \rho)^4} \exp \left(\frac{-4}{2 - \rho} \right)$$

Reference: Hillert, Mats. "On the theory of normal and abnormal grain growth." Acta metallurgica 13.3 (1965): 227-238.
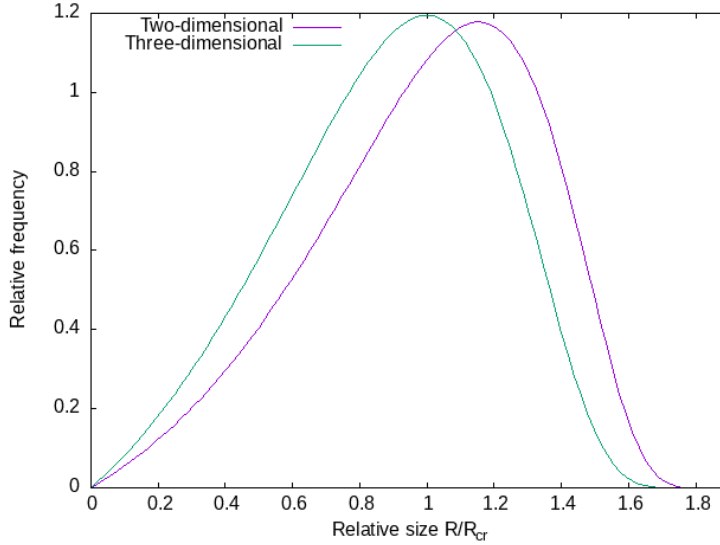
Figure 4.13: Hillert distribution in 2D and 3D.

4.6 Interface between two different phases

4.6.1 Coherent interfaces

The lattice parameter is generally different, when the interface is fully coherent (two crystals match perfectly) as shown in Fig. 4.14 and the magnitude of misfit strain (more comprehensively eigenstrain) is function of difference between difference of lattice parameters α and β phase. The interfacial energy of the coherent interface can be represented by γ_{ch}, which is approximately $200\,\text{mJ/m}^2$. The misfit strain is typically written by

$$\varepsilon_{ii}^0(\mathbf{r}) = \frac{a^\alpha - a^\beta}{a^\alpha} f(\mathbf{r})$$

where a^α is the lattice parameter of matrix phase and a^β is the lattice parameter of precipitated phase. $f(\mathbf{r})$ function is 1 in β phase and 0 in α phase. Without detailed discussion, elastic strain, $\varepsilon_{ij}^{\text{el}}(\mathbf{r})$ is given by

$$\varepsilon_{ij}^{\text{el}}(\mathbf{r}) = \varepsilon_{ij}(\mathbf{r}) - \varepsilon_{ij}^\circ(\mathbf{r})$$

where $\varepsilon_{ij}(\mathbf{r})$ is total strain and the elastic (strain) energy in coherent interface energy is

$$\gamma_{\text{el}} = \frac{1}{2} C_{ijkl}(\mathbf{r}) \varepsilon_{ij}^{\text{el}}(\mathbf{r}) \varepsilon_{kl}^{\text{el}}(\mathbf{r})$$

We generally assume that interface energy of the coherent interface can decompose into two terms

$$\gamma_{\text{ch}} = \gamma_{\text{grad}} + \gamma_{\text{el,ch}}$$

where γ_{grad} term is associated with concentration gradient. 'ch' subscript emphasize that it is the elastic energy of the coherent interface. For isotropic materials, we can assume that

$$\varepsilon_{11}^\circ(\mathbf{r}) = \varepsilon_{22}^\circ(\mathbf{r}) = \varepsilon_{33}^\circ(\mathbf{r}) = \varepsilon$$
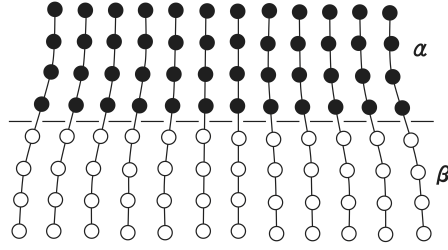
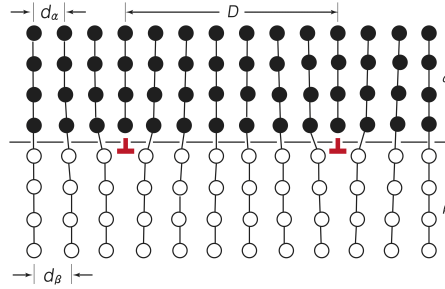Figure 4.14: Fully coherent interface with lattice mismatch.

Figure 4.15: Semi coherent interface with lattice mismatch and interface dislocation.

inside the precipitated phase. For isotropic materials, we generally say that

$$\gamma_{\mathrm{el}} = 4\mu\varepsilon^2 \tag{4.1}$$

where μ is shear modulus, which is unit of

$$\mathrm{Pa} = \mathrm{J/m}^3$$

.

4.6.2 Semicoherent interfaces

When magnitude of the misorientation (ε) increases, the elastic energy is too high to afford. As shown in Fig. 4.15, in the presence of the interface dislocation, lattice distortion can be reduced. With presence of the interface dislocation, not all atomic planes are coherent, therefore, we classify this type of the interface as the semicoherent interface. The semicoherent interface energy (γ_{sch}) can be represented by

$$\gamma_{\mathrm{sch}} = \gamma_{\mathrm{grad}} + \gamma_{\mathrm{el,sch}} + \gamma_{\mathrm{dc}}$$

where γ_{dc} is the dislocation core energy. In terms of the thermodynamics, the transition between coherent interface to the semicoherent interface occurs when

$$\gamma_{\mathrm{el,ch}} < \gamma_{\mathrm{el,sch}} + \gamma_{\mathrm{dc}}$$

with assumption that gradient energy does not depend on the type of interface. The typical value of the semicoherent interface is $200\,\mathrm{mJ/m}^2$-$500\,\mathrm{mJ/m}^2$.
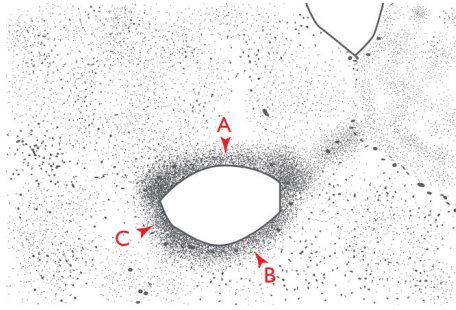
Figure 4.16: An α precipitate at a grain boundary triple point in an $\alpha-\beta$Cu-In alloy. A, B interfaces are coherent interface and C interface is semicoherent interface.
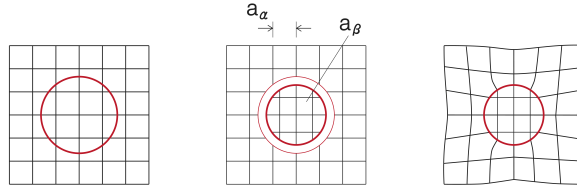

Figure 4.17: The origin of misfit strain between precipitate and matrix.

4.6.3 Incoherent interfaces

For incoherent interface, since there is no coherency across the interface, elasticity is not present for the case of incoherent interface. Only presence of the gradient energy is assumed and typical range of the energy is above $500 \, \text{mJ/m}^2$.

4.7 Morphology of precipitate

In solid state materials, different type of phase present in the limited region, we classify it as precipitate in the view point of microstructure. Comparing interface between matrix(βCu-In) and precipitate (β) in Fig. 4.16, semicoherent interface is relatively straight whereas coherent interface is curved. With assumption of isotropic crystal structure, the volumetric elastic energy can be estimated from Eq. 4.1.

$$\Delta G_{\text{el}} = 4\mu\varepsilon^2 V$$

where V is the volume of the precipitate. The misfit strain by the precipitate by lattice mismatch is illustrated in Fig. 4.17. Since the gradient term of the concentration and other structural parameters associated with surface, volumetric interface energy between spherical precipitate (radius r) and matrix phase is

$$\Delta G_{\text{int,ch}} = 4\mu\varepsilon^2 \cdot \frac{4}{3}\pi r^3 + 4\pi r^2 \cdot \gamma_{\text{grad}}$$

For semicoherent interface,

$$\Delta G_{\text{int,sch}} = 4\pi r^2 \cdot (\gamma_{\text{grad}} + \gamma_{\text{dc}})$$

since the interface dislocation is placed on the surface. Therefore, we expect that there can be transition from the coherent interface to the semicoherent interface as shown in Fig. 4.18.
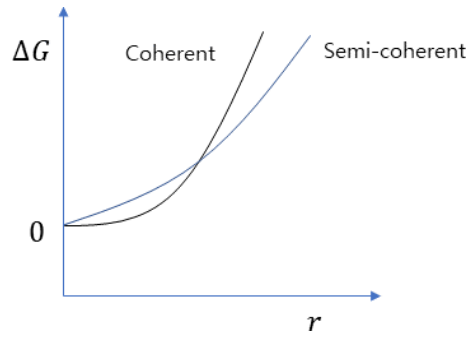
Figure 4.18: Schematic plot of interface energy with respect to radius r for coherent and semi coherent interface.